The 2009 IEEE/RSJ International Conference on
Intelligent Robots and Systems
October 11-15, 2009 St. Louis, USA

A Novel Piezoelectric Driven Laparoscopic Instrument with Multiple Degree of Freedom Parallel Kinematic Structure

A. Röse, C. Wohlleber, S. Kassner, H. F. Schlaak, R. Werthschützky

Abstract— **The development of a novel actuator driven laparoscopic instrument with parallel kinematic instrument tip serves to overcome the workspace restrictions of classic laparoscopic instruments and provides the surgeon multiple degrees of freedom (DOF) inside the patients body.**

First of all the requirements concerning control and motion have been derived in cooperation with medical partners. According to this, the aim of the project is to provide an intuitively controllable instrument especially suitable for laparoscopic dissection. It contains a 4-DOF movement at its intracorporeal side and can be one-hand-controlled by the surgeon. With 4 intracorporeal DOF it is possible to accomplish precision movements in a small intracorporeal workspace under different orientations.

A parallel kinematic mechanism for the moving instrument tip has been designed. This paper describes the development of the mechanism topology and a numeric approach for the kinematic calculation. To drive the mechanism during tissue manipulation forces of up to 15 N are required. Only piezoelectric drives provide a sufficient power density regarding forces and speed. Hence traveling wave ultrasonic motors have been chosen. The position and velocity control of a single motor is presented as well as the entire instrument control structure containing trajectory planning of the surgeons input and the kinematic calculation. An intuitive control is assured by a 3-DOF joystick that can be controlled by the surgeon's thumb.

A first prototype of the entire instrument has been successfully tested in an animal experiment.

I. Introduction

A. Restrictions of Laparoscopic Interventions

Minimally invasive therapies gain more and more importance in surgery because of the obvious benefits for the patients and the national healthcare systems - less trauma and less time spent in hospital. Laparoscopy is the term used for the minimal interventions in the abdomen. Surgeons working laparoscopically have to develop special operation skills since their workspace is limited to four degrees of freedom by the pivot point where the instrument enters the human body (Fig. 1). Thus much research work is done in the field of laparoscopic surgery in order to make instruments more flexible.

B. State of Research and Technology

One of the approaches that combine a motor driven instrument tip and an easy to use one-hand control is the one presented by Nakamura et al. [1]. Another flexible tool is availabe with the DaVinci™ EndoWrist™ [2]. These instruments are driven by cables through actuators that are situated apart from the instrument itself and provide a 2-DOF movement at the instrument tip (bending laterally to the instrument's longitudinal axis). Cable driven mechanics suffer from the fact that cables are difficult to sterilize and can only transmit pulling forces. Thus linear movements require complex mechanics and movements in a distinct 3-dimensional workspace are difficult to realize.

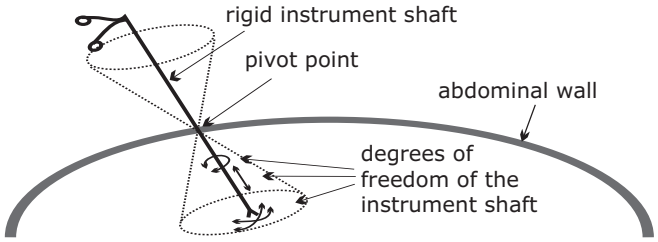

Fig. 1. Limited workspace due to mechanical restrictions in laparoscopy

In this paper we present a more flexible instrument using a parallel kinematic structure. It can move in a small intracorporeal workspace (4 DOF). It thus provides the possibility of accomplishing small precision movements even when the instrument shaft is fixed relatively to the body. This is especially helpful when a surgeon wants to cut tissue with a dissection instrument in a complex trajectory. Driven by actuators situated in the instrument itself the instrument tip can either be controlled by a 3-DOF joystick or be controlled to execute pre-programmed cutting movements. Another advantage of the presented parallel kinematic mechanism is its simple production due to the use of simple joints that can lead to low cost disposable instrument tips. In this paper the instrument tip is referred to as the tool center point (TCP).

C. Requirements

In an extensive study the requirements of laparoscopically working surgeons have been derived. Concerning the forces on the tool center point an instrument was equipped with a 3-DOF force sensor and has been used by surgeons on ex-vivo tissue in a cholecystectomy scenario. The experiments have shown that forces of up to 5 N occur at the tool tip [3]. The presented instrument has to stand these forces. The requirements for mobility and speed of the tool tip have been determined on the one hand by an interrogation of laparoscopically working surgeons and on the other hand by a scenario analysis of a minimally invasive resection of a small part of the liver. During the scenario analysis

This work was supported by the German Federal Ministry of Education and Research under grant 16SV2023

A. Röse, C. Wohlleber, S. Kassner, H. F. Schlaak, R. Werthschützky are with the Institute of Electromechanical Design, Department of Electrical Engineering and Information Technology, Technische Universität Darmstadt, 64283 Darmstadt, Germany a.roese@emk.tu-darmstadt.de

the surgeon explained which tools he would use for each step of the intervention. In most cases surgeons requested a bending of the instrument to work around the corner. An intracorporeal moving capability with at least 3 degrees of freedom (DOF) and working angles of up to 90° are requested. The TCP should be positionable within several cubic centimetres to accomplish small precision movements even when the instrument shaft is fixed relatively to the abdomen. The intracorporeal side of the instrument basically has to provide additional rotational degrees of freedom for working in different directions without changing the abdominal access. Moving velocities at the TCP can be relative slow ($v \leq 20\ \mathrm{mm/s}$) and accelerations should be high enough to provide a fast response to the surgeons trajectory input. With $a \geq 200\ \mathrm{mm/s^2}$ the final velocity of the instrument tip can be reached in $100\ \mathrm{ms}$, which will be sufficient.

II. Overview of the Instrument

The entire instrument concept is shown in Fig. 2. It is designed as a haptic telemanipulator. The upper branch - the telemanipulation - is object of this paper. A position sensing control element, the control and an intracorporeal platform consisting of actuators and a parallel kinematic mechanism have been designed and built as a prototype. The whole instrument concept is compatible with the lower branch - the haptic feedback - which is adressed in current and future work [4]. The instrument shall be used by a surgeon just the same way as a classic laparoscopic instrument leading to the design of a handheld device. Fig. 3 gives a short overview of the intended use of the laparoscope. As an example for a surgical tool a laser dissector for cutting tissue is implemented.

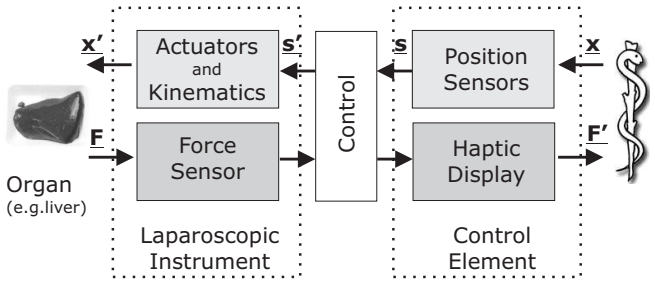

Fig. 2. Block-diagram of the presented instrument. The telemanipulation is already implemented. The haptic feedback is objective of current work.

III. Kinematic structure

A. Development of the mechanism

1) Overview of the motion capabilities: According to the requirements a serial kinematic chain of the intracorporeal part of the instrument has been defined as shown in Fig. 4. The combination of two rotational DOF θ_1 and θ_2 and one linear DOF q_1 guarantees a workspace of some cm^3 that can easily be controlled by a 3-DOF Joystick (θ_1: tilt, θ_2: pan, q_1: move forward/backward). The 4^{th} DOF θ_3 is a rotational hinge that extends the rotational capability to one side. This provides a total deflection of 80° to one side of the

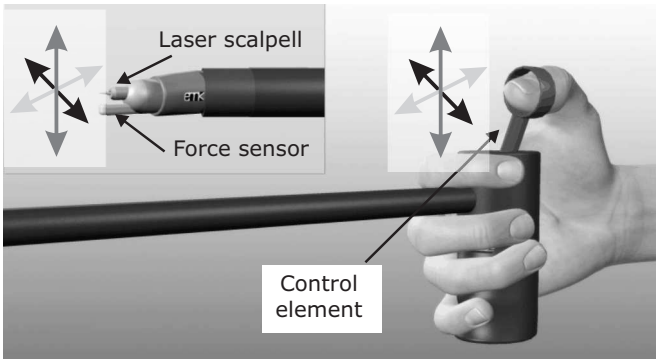

Fig. 3. Use-case scenario. The instrument tip is moving according to the input at the control element. A LASER-scalpel has been used for cutting tissue.

Instrument. This serial kinematic chain is referred to as the *"main kinematic chain"*. As the user shall control the joints $\theta_{1,2,3}$ and q_1 the easiest kinematic structure would result by placing actuators in these joints. Actuators of that small size at the required forces, are not available. Thus the actuators will be placed in the instrument shaft and the development task is to provide a parallel kinematic mechanism, which contains the above presented *main kinematic chain* and provides motions according to Fig. 4. Additionally it shall be stretched "finger like" but also well resist lateral forces.

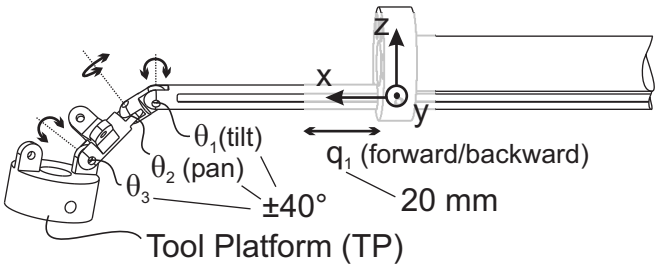

Fig. 4. *Main kinematic chain* of the instrument tip. The motion capabilities of this chain determine the motion of the whole parallel kinematic mechanism. The parallel kinematic mechanism has to be designed such, that it can actuate the joints of the *main kinematic chain*.

2) Parallel kinematic mechanism design: A parallel mechanism with 4 DOF generally consists of 4 kinematic chains with one actuator in each chain. Here the first kinematic chain is given by the *main kinematic chain*, as it determines the desired motion. One of the remaining chains is connected directly to the Tool Platform (TP). The 2 remaining chains are connected to the *main kinematic chain* in between the base and the TP to form a fully parallel substructure. By doing this, the mechanism becomes stiffer against lateral forces. This approach leads to the kinematic scheme shown in Fig. 5. The degrees of relative motions to be permitted by all the joints in the mechanism, can be calculated by the loop mobility criterion [5]:

$$\sum f_i = F + 6 \cdot L = 4 + 6 \cdot 3 = 22 \qquad (1)$$

Where $\sum f_i$ is the sum of relative motions to be permitted by the joints in the mechanism, F is the number of DOF of

the mechanism, which is 4 in our case and L is the number of independent loops, which is 3 in our case.

Four relative joint motions are already placed in the *main kinematic chain*, 18 DOF remain to be placed. They are equally distributed on the remaining three chains (Fig. 5). With one actuator per chain fixed to the base, this mechanism can be actuated in 4 DOF according to the restrictions of the *main kinematic chain*.

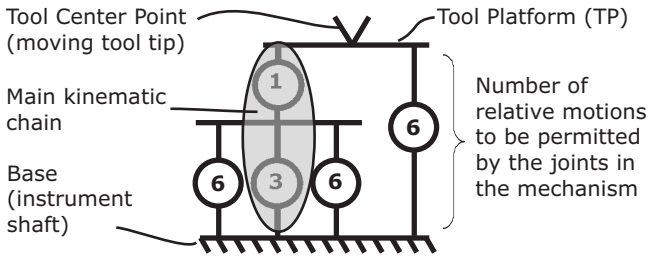

Fig. 5. Kinematic scheme of the parallel kinematic mechanism

3) Realization and Workspace: Fig. 6 shows the first functional sample as a result of the design process. Four driving rods move in the direction of the instrument shaft while the TP carrying the manipulation instrument moves within the orientated workspace shown in Fig. 7. The small arrows point into the working direction while their bases represent the TCP position. The workspace is obtained from the analysis of the mobility of the *main kinematic chain*.

The passive joints are distributed as 1-DOF rotational joints to simplify their fabrication and assembly and to later allow the manufacturing of the whole mechanism as one injection molded part with flexible hinges. An $11\ \mathrm{cm}^3$ workspace has been achieved with a $80°$ working angle in tilt direction. Surgeons often perform complex cutting geometries by successive small movements. That is possible with the presented mechanism even when the instrument shaft is fixed relatively to the patient.

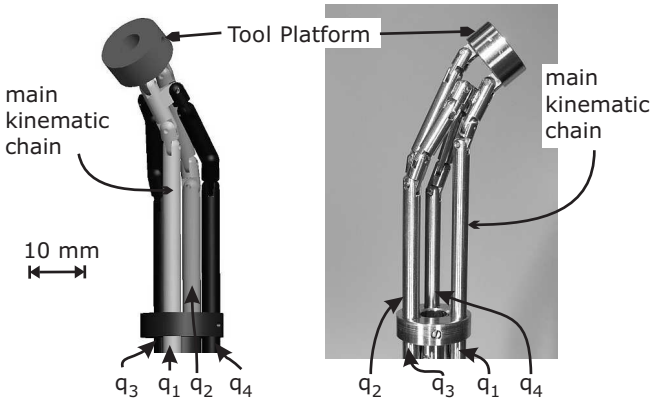

Fig. 6. First functional sample of the parallel kinematic mechanism. The actuators $q_{1,2,3,4}$ drive the parallel kinematic mechanism

B. Kinematic Calculation

As mentioned above, the passive joints are all designed as revolute joints due to fabrication reasons. This restriction

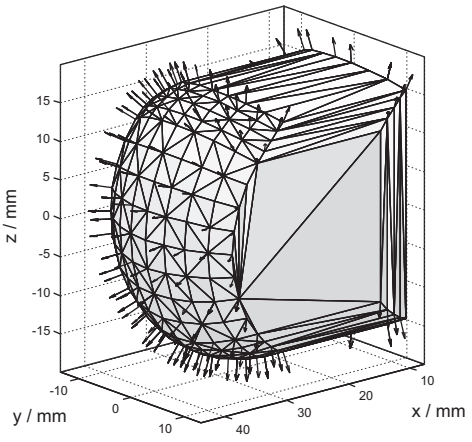

Fig. 7. Workspace of the presented mechanism as a convex hull with small arrows pointing in the working direction. The workspace is orientated according to the coordinate system in Fig. 4

is important to simplify the production of the mechanism but it makes the inverse kinematic calculation more complex than for mechanisms with spherical joints or universal joints. In order to obtain an analytical solution for the inverse kinematic problem of a parallel mechanism the inverse kinematic problem for every serial kinematic chain has to be solved. As this solution here would be very complex a numeric solution is presented. The numeric solver does not provide the Jacobian model of the mechanism. Thus singularity analysis has to be done with different methods. A numeric multi body simulation tool (e.g. Simulink® SimMechanics™) can be used for singularity analysis.

In the case of the given mechanism, one intuitive way for the surgeon to control the instrument TCP is to control the joints in the *main kinematic chain* (refer to Fig. 4: q_1: move forward/backward, θ_1: tilt, θ_2: pan, θ_3: preset of a working angle). That is the way the manual control of the instrument is implemented (Fig. 3). The numeric solver has to find an assembled configuration of the parallel mechanism for a position of the *main kinematic chain* given by the user. Due to the design according to (1), this assembled configuration is unique in a singularity-free workspace and contains a unique position for the actuators ($q_{1,2,3,4}$), and thus the desired solution. The solver derives a solution for:

$$\mathbf{q} = f(q_1, \theta_1, \theta_2, \theta_3) \tag{2}$$

where $\mathbf{q}$ is the solution for the position vector of the actuators $q_{1,2,3,4}$ for a given position of the *main kinematic chain* $(q_1, \theta_1, \theta_2, \theta_3)$

The numeric solver works as follows: The position and orientation of all other kinematic chains are modified by a Gauß-Newton algorithm to minimize their distance to the *main kinematic chain*. The example shown in Fig. 8 gives

$$g(q_3, \varphi_1, \varphi_2, \varphi_3, \varphi_4, \varphi_5) - h(q_1, \theta_1, \theta_2, \theta_3) \rightarrow min, \tag{3}$$

where $g(q_3, \varphi_1, \varphi_2, \varphi_3, \varphi_4, \varphi_5)$ is the position and orientation of one kinematic chain and $h(q_1, \theta_1, \theta_2, \theta_3)$ is the (given) position and orientation of the *main kinematic chain*. After

minimization of (3) an assembled position for the kinematic chain in Fig. 8 is found.

The numeric solver presents a solution every $1-2\mathrm{ms}$ on a Pentium 2 GHz processor running under Windows. This is due to the fact that the approximation starts from the last calculated solution. The last solution is "not far away" from the new solution regarding realistic velocities. For the current application this is fast enough. The solver is implemented in $\mathrm{LabView}^{\circledR}$. The calculation speed can be increased using dedicated calculation hardware e.g. field programmable gate arrays (FPGA) [6].

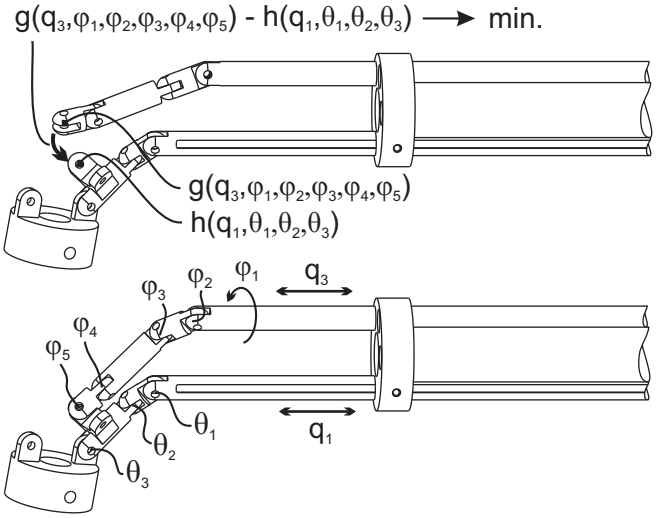

Fig. 8. Functionality of the numerical kinematic solver. When a new position of the *main kinematic chain* is set, the solver minimizes the distance (and orientation) between all chains and the *main kinematic chain* by adjusting all joints of the other chains. Thus a solution for all passive joints and more important for the displacement of the actuators $q_{2,3,4}$ is found.

IV. Actuation and Control Structure

A. Piezoelectric Actuation

1) Requirements: As mentioned in the requirements section (I-C) for laparoscopic interventions the instrument tip has to resist forces of up to 5 N. Assuming a (realistic) force transmission ratio of the parallel kinematic mechanism of $0.3\ldots3$ in its workspace, forces of up to 15 N can occur at the actuators. The motion speed scales up to $60\ \mathrm{mm/s}$ at the actuators in the worst case. Following the requirements, the actuators have to achieve accelerations of up to $600\ \mathrm{mm/s^2}$.

Due to the idea to integrate the actuators in the instrument shaft, actuators with high power density are required. Miniature DC motors provide enough power but require bulky gearboxes to reduce their speed. Piezoelectric motors deliver high torque at low speed and are well suited for this application [7].

2) Traveling Wave Ultrasonic Motors: The Shinsei USR30 is a traveling wave ultrasonic motor (TWUSM). A flexural wave is piezoelectrically generated and propagates on the stator. The rotor is strongly pressed onto the stator and is actuated by the elliptical motion of the contact points. As the motor is driven by the ultrasonic resonant frequency of the stator it can develop higher force than stepper motors, has high dynamic response and remains almost silent. With $50\ \mathrm{mNm}$ at $30\ \mathrm{mm}$ diameter, $9\ \mathrm{mm}$ height and $20\ \mathrm{g}$ it shows a high power density. These features make it very promising for laparoscopic instruments. The prototype of the instrument integrates 4 of these motors in its extracorporeal shaft. The linear motion needed by the parallel kinematic instrument tip is provided by a rack and pinion mechanism (Fig. 9). With a radius of $3.5\ \mathrm{mm}$ the torque of the motor is transformed to about $14\ \mathrm{N}$ at the driving rods.

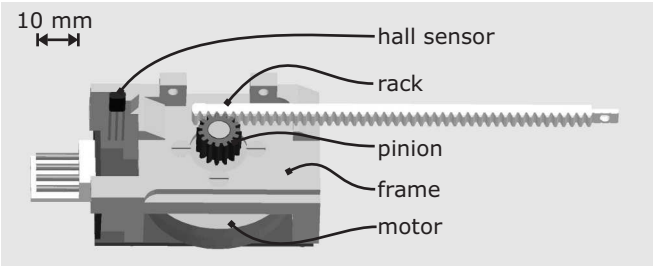

Fig. 9. Design drawing of a motor module

B. Control

1) Actuator Position Control: The major drawback of the TWUSM is that it is difficult to control. The torque is nonlinear and varies with the speed, load and temperature. It is necessary to model the behavior of the motor to achieve precise and stable position control. The electromechanical equivalent circuit [8] is a simple way to describe the characteristics of the motor. However, it cannot model the contact between stator and rotor accurately and is only valid for steady state operation. An analytical model based on Hamilton's principle can be combined with contact mechanics theory for the complete description of the motor [9]. Yet the accurate parameters of these models are hard to obtain. The derivation of a control law is difficult because of their nonlinearity. A simplified model taking most characteristics into account while being easy to implement is presented in [10]. If the rotor is supposed ideal and no slip is assumed at the contact to the stator, then the angular velocity of the ideal rotor is proportional to the wave amplitude W:

$$\dot{\Theta}_{id} = \omega \frac{kh}{b^2} W \tag{4}$$

where ω is the angular frequency of the traveling wave. k, b and h are the wave number, radius and thickness of the stator. The contact is then modeled as a friction torque

$$T = f_0[\dot{\Theta}_{id} - \dot{\Theta}] \tag{5}$$

where f_0 is the friction coefficient, $\dot{\Theta}$ is the actual angular velocity of the motor and $\dot{\Theta}_{id}$ is the ideal angular velocity.

Near the resonance, the traveling wave amplitude can be tuned by the driving frequency. As the amplitude can be monitored by a feedback electrode which is situated on the stator, it can be controlled in a first loop (Fig. 10). Then the

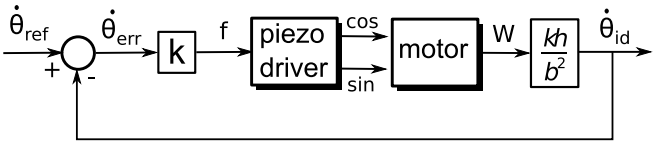

Fig. 10. Wave amplitude control loop

motor position is controlled in a second loop to compensate the load variations and the uncertainties of the model. The position control is done separately for each motor as the kinematic calculation is computed on external hardware. The commands of the surgeon are transformed in linear position commands for each of the 4 driving rods. The position feedback is given by an incremental magnetic encoder at the rear of the rotor. The absolute position is referenced at the beginning of the operation with a hall sensor that detects a permanent magnetic strip placed on the driving rod.

2) Instrument Control and Trajectory Planning: To follow smoothly and accurately the commands of the surgeon, it is necessary to control both, the position and the velocity of the motors. Each DOF is controlled by a P-position/PI-velocity loop. A PI-velocity loop is enclosed within a proportional position loop. The velocity is estimated from the position signal by differentiation and low-pass filtering to remove the quantization noise from the encoder. As the surgeon's control input is not known in advance, online trajectory planning is necessary (Fig. 11). First, the movements of the surgeon's thumb are taken from the manual control element and are sampled into key trajectory points of the movement of the *main kinematic chain*. Then the motor positions (here p_1 and p_2) at these points are calculated with the kinematic solver from equation (2). The motors have to pass through these control points with defined velocities (v_1 and v_2 respectively). Then, the low-level position and velocity commands are generated at full control loop rate for the motor controllers. To achieve this, a trapezoidal velocity

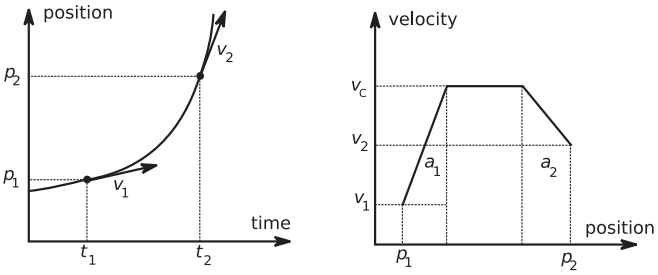

Fig. 11. Trajectory planning; left: movements of the surgeon with two key points; right: computed velocity profile

profile is extracted from the key trajectory points to limit the maximum velocity and acceleration of the motors. The 3 phases of the profile, constant acceleration a_1, cruising at velocity v_C and constant deceleration a_2 are generated to reach the key points at the defined time and with the correct velocity. The implementation as a velocity feed-forward (Fig. 12) improves the command response and corrects the trajectory following error of the P/PI-loop. This online trajectory computation [11] is also used to synchronize the 4 motors. The trajectory of the slowest motor is first computed and the speed of the other motors adapted accordingly. As the motors are controlled separately, the synchronization of the rods is critical for the trajectory of the manipulation platform.

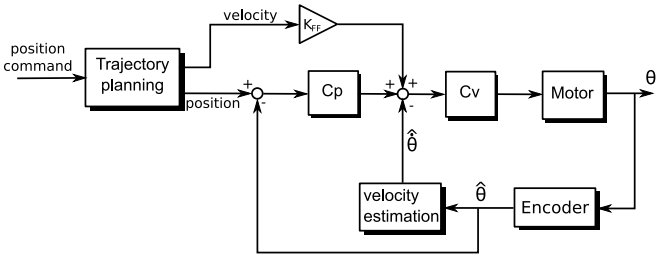

Fig. 12. Position control. Cp: position controller, Cv: velocity controller, K_{FF}: feed-forward gain

3) Experimental Results: The control strategy has been tested in the instrument's prototype. The control loop runs at 500 Hz on a microcontroller. The position commands for each motor are computed by the kinematic calculation on a PC and provided with 50 Hz on a SPI bus. The controller outputs are sent to the motor drivers as an analog signal with a 4 channel DAC. Fig. 13 shows the response of the motor to a position change with trajectory planning. The velocity feed-forward provides a fast response of the input control and better tracking as no following error has to build up first. A small steady state error is observed, as the motor presents a dead zone at low speed. Tuning the wave amplitude with the phase of the driving signals in addition to their frequency should reduce the influence of the dead zone [10].

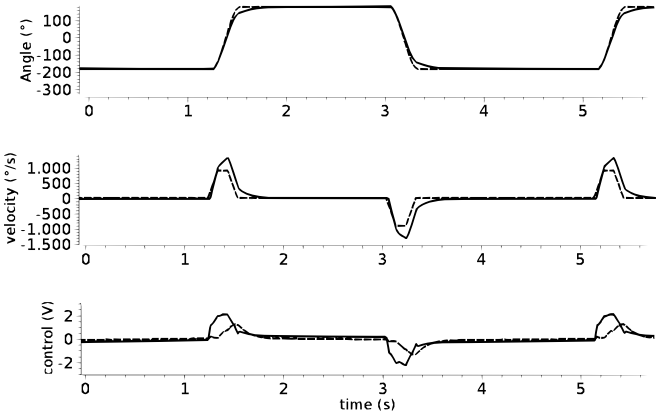

Fig. 13. Response of the motor to a position change with trajectory planning. In the angle and velocity diagrams, the dashed lines represent the calculated trajectory of the trajectory planner and the solid lines show the measured motor motion. The third diagram shows the difference of the motor control voltage with (solid line) and without (dashed line) velocity feed forward.

V. Assembly and Animal Experiment

The disassembled device is presented in Fig.14. The whole instrument is mounted with one single screw simplifying the use and cleaning. The presented instrument has been built

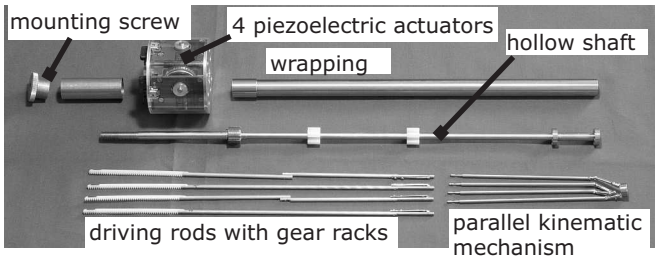

Fig. 14. Disassembled instrument. Mounting the parts is done with one single mounting screw.

and tested in an in-vivo animal experiment on a pig. Fig. 15 shows the experimental setup. The surgeon holds the device just like a normal laparoscopic instrument. The actuators are situated outside the body near the control element. In the experiment a wedge could simply be cut out of the liver. A video of the instrument handling and the animal experiment can be downloaded on IEEE Xplore.

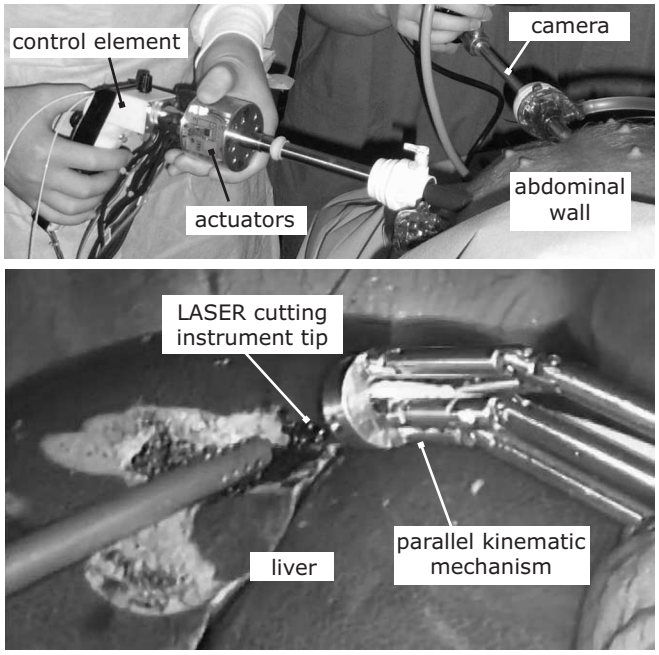

Fig. 15. Animal experiment with the described instrument. A wedge is cut out of a porcine liver with a laser dissector

VI. Conclusion and future works

A laparoscopic instrument with 4 degrees of freedom and intuitive control has been designed and realized. It uses piezoelectric drives for strong and fast movements. A 4-DOF parallel kinematic instrument tip, that is potentially low cost producible due to its simple joint structure, has been designed and built as a functional sample. A 3-DOF joystick has been provided. It allows an intuitive control in a small workspace even when the instrument itself is fixed relatively to the patient. The 4^{th} DOF of the instrument tip, an additional working angle, can be preset. The parallel kinematic mechanism is designed to fit surgical requirements regarding the moving capabilities. The real time kinematic calculation is done numerically. The whole instrument has been successfully tested by surgeons in an animal experiment.

A force sensor, measuring the interaction force with the tissue in 3 dimensions and an active control device, needed for haptic feedback, are under development. Due to the control philosophy the intuitive 3-DOF control is compatible with a 3-DOF force feedback.

VII. Acknowlegements

We want to thank the German Federal Ministry of Education and Research for supporting the INKOMAN project under the reference number 16SV2023. Special thanks are devoted to our medical partners at Universitätsklinikum Schleswig-Holstein - Campus Lübeck and at Universitätsklinikum Hamburg-Eppendorf as well as our engineering partners at Bauer & Häselbarth - Chirurg GmbH and at Institut für Biomedizinische Optik in Lübeck.

References

[1] R. Nakamura, T. Oura, E. Kobayashi, I. Sakuma, T. Dohi, N. Yahagi, T. Tsuji, M. Shimada, and M. Hashizume, "Multi-dof forceps manipulator system for laparoscopic surgery - mechanism miniaturized evaluation of new interface -," in *MICCAI '01: Proceedings of the 4th International Conference on Medical Image Computing and Computer-Assisted Intervention*. London, UK: Springer-Verlag, 2001, pp. 606–613.

[2] G. Guthart and J. Salisbury, "The Intuitive TM telesurgery system: Overview and application," *IEEE ICRA, San Francisco, CA*, 2000.

[3] J. Rausch, A. Röse, R. Werthschützky, and H. F. Schlaak, "Analysis of mechanical behavior of liver tissue during intracorporal interaction," in *Biomedizinische Technik. Proceedings. Gemeinsame Jahrestagung der Deutschen , Österreichischen und Schweizerischen Biomedizinische Technik*, ETH Zürich, 2006.

[4] S. Kassner, J. Rausch, A. Kohlstedt, and R. Werthschützky, "Analysis of mechanical properties of liver tissue as a design criterion for the development of a haptic laparoscopic tool," in *4th European Congress for Medical and Biomedical Engineering 2008. Proceedings.*, Antwerp, Belgium, 2008.

[5] L.-W. Tsai, *Robot Analysis and Design: The Mechanics of Serial and Parallel Manipulators*. New York, NY, USA: John Wiley & Sons, Inc., 1999.

[6] D. Hildenbrand, H. Lange, F. Stock, and A. Koch, "Efficient inverse kinematics algorithm based on conformal geometric algebra using reconfigurable hardware," in *Intl. Conf. on Computer Graphics Theory and Applications (GRAPP)*, Funchal, 01/2008 2008.

[7] T. Morita, "Miniature piezoelectric motors," *Sensors and Actuators A: Physical*, vol. 103, no. 3, pp. 291 – 300, 2003.

[8] L. Petit, N. Rizet, R. Briot, and P. Gonnard, "Frequency behaviour and speed control of piezomotors," *Sensors & Actuators: A. Physical*, vol. 80, no. 1, pp. 45–52, 2000.

[9] N. El Ghouti, "Hybrid Modeling of a Traveling Wave Piezoelectric Motor," Ph.D. dissertation, Dep. of Gontrol Engineering Aalborg University, 2000.

[10] F. Giraud, B. Lemaire-Semail, J. Aragones, J. Robineau, and J.-T. Audren, "Precise position control of a traveling-wave ultrasonic motor," *IEEE Transactions on Industry Applications*, vol. 43, no. 4, pp. 934 – 941, 2007.

[11] T. Kroger, A. Tomiczek, and F. Wahl, "Towards on-line trajectory computation," in *2006 IEEE/RSJ International Conference on Intelligent Robots and Systems*, Beijing ISBN: 1-4244-0259-X, 2006, pp. 736 – 741.